CrossMark

Impact of land cover characterization on regional climate modeling over West Africa

Mouhamadou Bamba Sylla[1,2] · Jeremy S. Pal[2] · Guiling L. Wang[3] · Peter J. Lawrence[4]

Abstract The impact of high resolution modern vegetation cover on the West African climate is examined using the International Centre for Theoretical Physics Regional Climate Model implementing the NCAR Community Land Model. Two high resolution 25 km long-term simulations driven by the output from a coarser 50-km resolution simulation are performed for the period 1998–2010. One high resolution simulation uses an earlier and coarser-resolution version of plant functional type distribution and leaf area index, while the other uses a more recent, higher-quality, and finer-resolution version of the data. The results indicate that the new land cover distribution substantially alters the distribution of temperature with warming in Central Nigeria, northern Gulf of Guinea and part of the Sahel due to the replacement of C4 grass with corn; and cooling along the coastlines of the Gulf of Guinea and in Central Africa due to the replacement of C4 grass with tropical broadleaf evergreen trees. Changes in latent heat flux appear to be largely responsible for these temperature changes with a net decrease (increase) in regions of warming (cooling). The improved land cover distribution also results in a wetter monsoon season. The presence of corn tends to favor larger precipitation amounts via more intense events, while the presence of tropical broadleaf evergreen trees tends to favor the occurrence of both more intense and more frequent events. The wetter conditions appear to be sustained via (1) an enhanced soil moisture feedback; and (2) elevated moisture transport due to increased low-level convergence in regions south of 10N where the most substantial land cover differences are present. Overall the changes induced by the improved vegetation cover improve, to some extent, the performance of the high resolution regional climate model in simulating the main West African summer monsoon features.

Keywords Regional climate modeling · Land cover distribution · Turbulent fluxes · West African summer monsoon climate

1 Introduction

West African monsoon (WAM) climate is characterized by strong interaction between ocean sea surface temperatures (SSTs), atmospheric circulation, and continental land surface conditions (Fontaine et al. 1998; Wang and Eltahir 2000; Giannini et al. 2003; Jenkins et al. 2005). Modeling this complex interplay between the monsoon and drivers is of primary importance for an accurate representation of precipitation over the Sahel and thus essential for a better understanding of the response of West African climate to increases in anthropogenic greenhouse gases (GHGs).

Recent modeling studies indicate that land surface changes significantly affect climate and ecosystems across the world (e.g., Koster et al. 2004; Patricola and Cook 2008; Abiodun et al. 2012; van den Hurk and van Meijgaard 2010; Alo and Wang 2010). Such influences are

✉ Mouhamadou Bamba Sylla
syllabamba@yahoo.fr; sylla.b@wascal.org

1 West African Science Service Center on Climate Change and Adapted Landuse (WASCAL), WASCAL Competence Center, 06 PO BOX 9705, Ouagadougou, Burkina Faso

2 Department of Civil Engineering and Environmental Science, Loyola Marymount University, Los Angeles, CA, USA

3 Department of Civil and Environmental Engineering, University of Connecticut, Storrs, CT, USA

4 Cooperative Institute for Research in Environmental Sciences, University of Colorado, Boulder, CO, USA

established through biogeochemical and biogeophysical interactions involving the carbon cycle, hydrological processes and exchange of energy and momentum through the atmospheric boundary layer (Bounoua et al. 2002; Kueppers et al. 2007). The West African region is particularly sensitive to such changes in surface conditions (e.g., Koster et al. 2004; Abiodun et al. 2008). This sensitivity originates from the dependence of the monsoon circulation and precipitation on the meridional low-level air temperature, soil moisture and potential vorticity gradients (Cook 1999; Hsieh and Cook 2005; Sylla et al. 2011). Land cover distribution, soil characteristics and soil moisture determine the partitioning of net solar radiation into latent and sensible heat fluxes (Feddema et al. 2005; Zaroug et al. 2012; Otieno and Anyah 2012). The resulting feedback strongly impacts the WAM circulation and precipitation (Xue et al. 2004; Steiner et al. 2009). For instance, Xue et al. (2004) showed that vegetation processes are important for WAM evolution affecting both the intensity and spatial extent of precipitation and the associated circulation. Likewise, Abiodun et al. (2010) argued that deforestation increases the intensity of the African Easterly Jet (AEJ) core, thus reducing the northward transport of moisture needed for precipitation over West Africa. Furthermore, Alo and Wang (2010) showed that dynamic vegetation feedback reverses the predicted future trend, leading to a substantial increase of annual rainfall. These studies emphasize the key role of land cover distribution in the land surface-climate interactions over West Africa.

A critical issue in simulating WAM precipitation is the existence of significant biases in climate models (Afiesimama et al. 2006; Konaré et al. 2008; Diallo et al. 2013; Nikulin et al. 2012; Gbobaniyi et al. 2014). This deficiency can originate from the inability of the models to realistically simulate large-scale conditions (Pohl and Douville 2011); respond adequately to such conditions via their convective parameterizations (Crétat et al. 2012); and from the quality of the various input data (Moufouma-Okia and Rowell 2010; Diro et al. 2012; Sylla et al. 2012a; Yu and Wang 2013). The quality of data used to specify land cover is likely to contribute to such biases via impacts to the surface energy and moisture budgets and consequentially temperature and precipitation.

Regional climate models (RCMs) are proven to be particularly valuable to simulate WAM climate (e.g., Afiesimama et al. 2006; Hourdin et al. 2010; Xue et al. 2010; Ruti et al. 2010; Diallo et al. 2012; Sylla et al. 2013a; Mounkaila et al. 2014). Their higher resolution allows for a better representation of fine-scale forcing and land surface heterogeneity such as complex topography, coastlines and land surface variations—all of which are important to accurately simulate the local and regional climate system (Paeth et al. 2005; Rummukainen 2010; Sylla et al. 2012b).
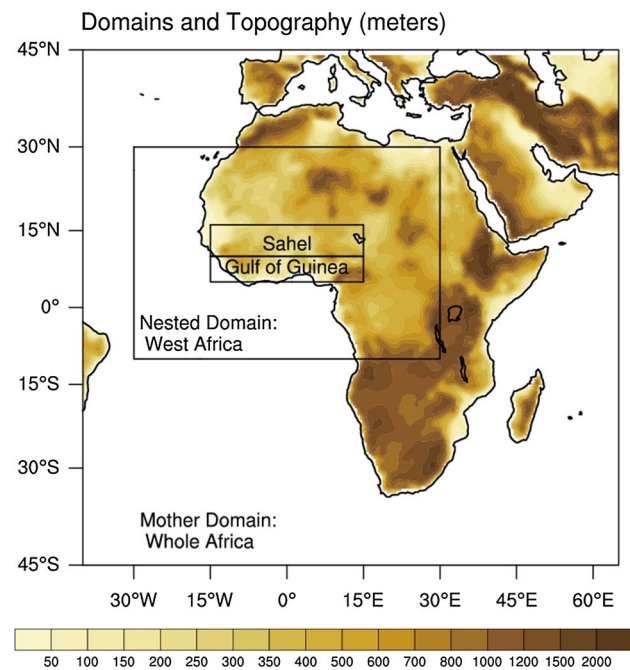

Fig. 1 Simulation domains and topography (m)

In this study, the International Centre for Theoretical Physics (ICTP) Regional Climate Model version 4.3 (RegCM4.3) coupled with the National Center for Atmospheric Research (NCAR) Community Land Model (CLM3.5) is applied to examine the influence of improved land cover distribution on the simulation of WAM climate. Experiments are performed with both the default coarse resolution vegetation and newer high resolution improved land cover. The model and design of numerical experiments are described in Sect. 2; the results are presented and discussed in Sect. 3; and final considerations are provided in Sect. 4.

2 Model description and experimental design

The ICTP RegCM4.3 is a primitive equation, sigma vertical coordinate limited area model (Giorgi et al. 2012). The version of RegCM4 in this study employs dynamics and physical parameterizations identical to those in RegCM3 (Pal et al. 2007). It is based on the hydrostatic dynamical core of the National Center for Atmospheric Research/Pennsylvania State University's Mesoscale Meteorological Model version 5 (NCAR/PSU's MM5; Grell 1993). Radiation is represented by the Community Climate Model version 3 parameterization of Kiehl et al. (1996) and the planetary boundary layer according to the Holtslag et al. (1990) formulation. The scheme of Zeng et al. (1998) is used to represent fluxes from ocean

Fig. 2 Difference in fraction of area (in %) between the improved PFT and the default PFT data for different plants
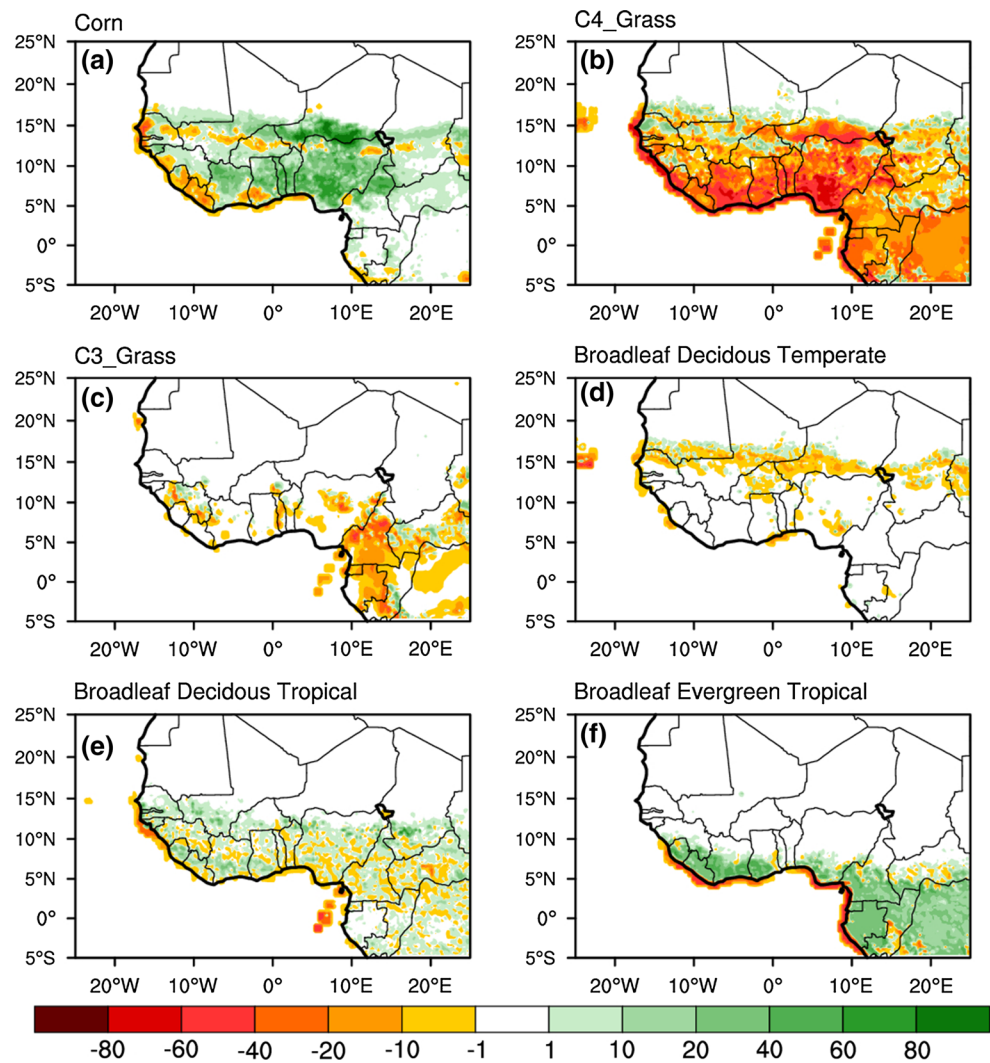

surfaces while convective precipitation is calculated with the Massachusetts Institute of Technology scheme (Emanuel 1991). Resolvable precipitation processes are treated with the Subgrid Explicit Moisture Scheme (SUBEX; Pal et al. 2000). Interactions between the land surface and the atmosphere are described using the Community Land Model CLM3.5 (Oleson et al. 2008). CLM3.5 is a state of the science land surface model with a physical representation of surface energy budget and water cycle. The model represents land surface heterogeneity using a hierarchical data structure. Each land grid cell can be divided into a different number of land units; each land unit can be divided into multiple soil/snow columns; each column can be occupied by multiple plant functional types (PFTs) that differ in physiology and structure. A total of 16 PFTs are considered in CLM3.5. In the vertical direction, a column consists of ten soil layers and up to five snow layers (depending on snow depth). Within each grid cell, all components share the same atmospheric forcing; the

surface fluxes (that are passed to the atmospheric model) are area-weighted averages among different components (PFTs, columns, and land units) within each grid cell. Of particular interest in this study is the representation of land cover in the land surface model.

To examine the effect of vegetation feedback on the simulation of WAM climate, three simulations for the period 1997–2010 are conducted over the region (Fig. 1). The first year of the simulation (1997) is considered as spin-up and is not included in the analysis. The mother domain simulation (hereafter referred to as MD) is performed at a 50-km grid spacing using the default CLM3.5 PFT data. The remaining two simulations are nested within the mother domain at a 25-km grid spacing, with the only difference being the specified PFT data: default $0.5 \times 0.5°$ PFT data (LoResDef) and the improved $10 \times 10'$ PFT data better reflecting the vegetation cover over West Africa (HiResNew; Lawrence and Chase 2010). Over West Africa, the primary differences between the two PFT datasets are

Fig. 3 Time-Latitude Hov-moller diagram of 2-meter monthly temperature (°C) averaged for the period 1998–2010 and between 15E to 15N for UDEL (*upper panel*), LoResDef (*middle panel*) and the bias (LoResDef minus UDEL: *lower panel*)
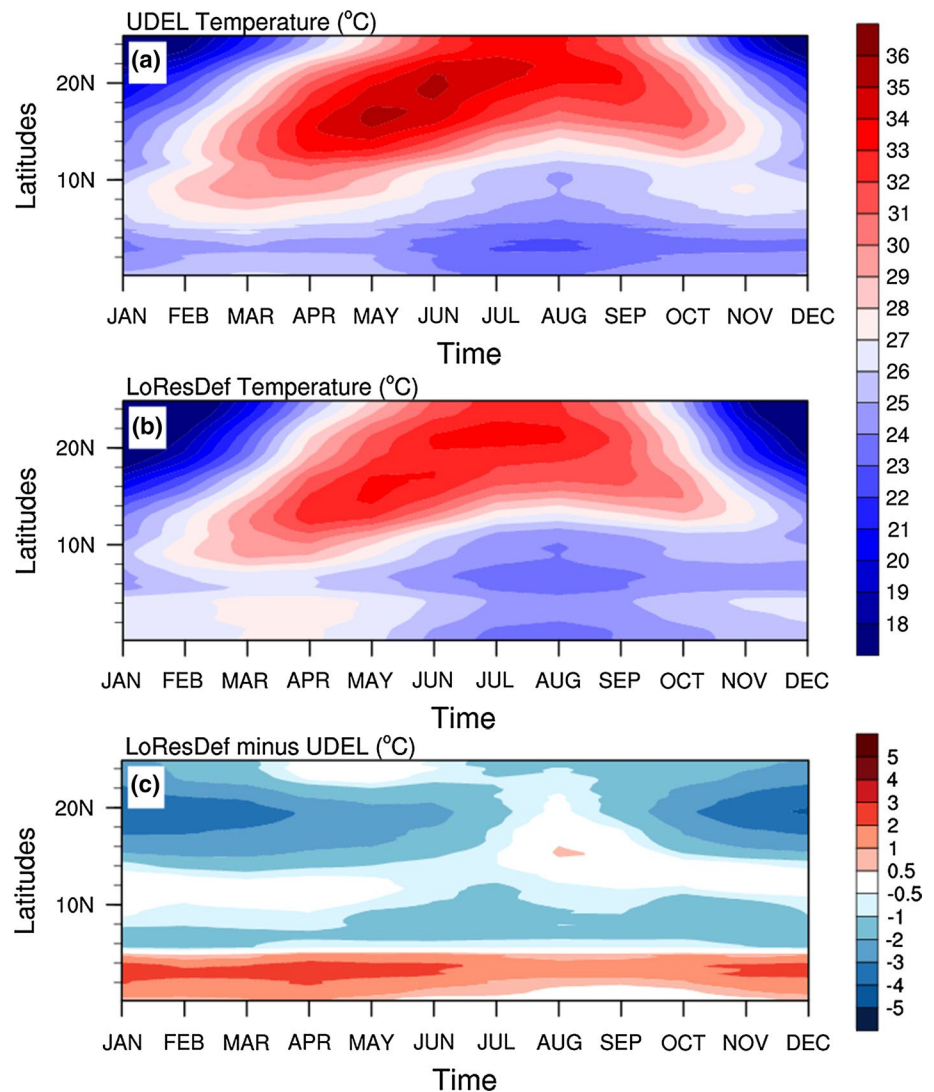
that most of the C4 and C3 grasses have been converted into corn in the Gulf of Guinea, Nigeria, and Northeastern Sahel and to tropical broadleaf evergreen trees over most of central Africa and a portion of the Gulf of Guinea (Fig. 2).

Initial and lateral boundary conditions used to drive RegCM4.3-CLM3.5 over the mother domain are derived from the ERA-Interim 1.5 × 1.5° 6-hourly third generation of European Centre for Medium Range Weather Forecasts (ECMWF) reanalysis product gridded reanalysis (ERA-Interim; Dee et al. 2011). SSTs for all experiments are obtained from the National Oceanic and Atmospheric Administration Optimum Interpolation weekly 1 × 1° grid dataset (Reynolds et al. 2002).

To examine the response of climate to the updated land cover, simulated precipitation and temperature from the experiments are compared to the gridded 0.5 × 0.5° monthly station-based observations from the University of Delaware (UDEL; Legates and Willmott 1990) and the

Climatic Research Unit (CRU TS 3.2.0; Harris et al. 2014). Due to the scarcity of meteorological station data in Africa, both the UDEL and CRU datasets are effectively coarser than the provided 0.5 × 0.5°. Despite this deficiency, however, many of the spatial and temporal characteristics of precipitation and temperature over Africa can be observed (especially with the UDEL data). To account for the lacking spatial coverage of the UDEL and CRU precipitation data, the daily and monthly 25 × 25 km satellite-gauge merged product of Tropical Rainfall Measuring Mission (TRMM; 3B42 version 7) are used for further model validation and provide coverage over oceans (Kummerow et al. 2001; Huffman et al. 2007). Two measures are used to quantify the model performance: the mean bias representing the area average difference between the simulations and observations; and the pattern correlation coefficient (PCC) measuring how well the simulations capture the distribution of spatial variations compared to observations.

Fig. 4 Mean December–February (DJF: *left panel*) and June–August (JJA: *right panel*) 2-m temperature (°C) for the period 1998–2010 from UDEL (*upper panel*), LoResDef (*middle panel*) and the bias (LoResDef minus UDEL: *lower panel*)
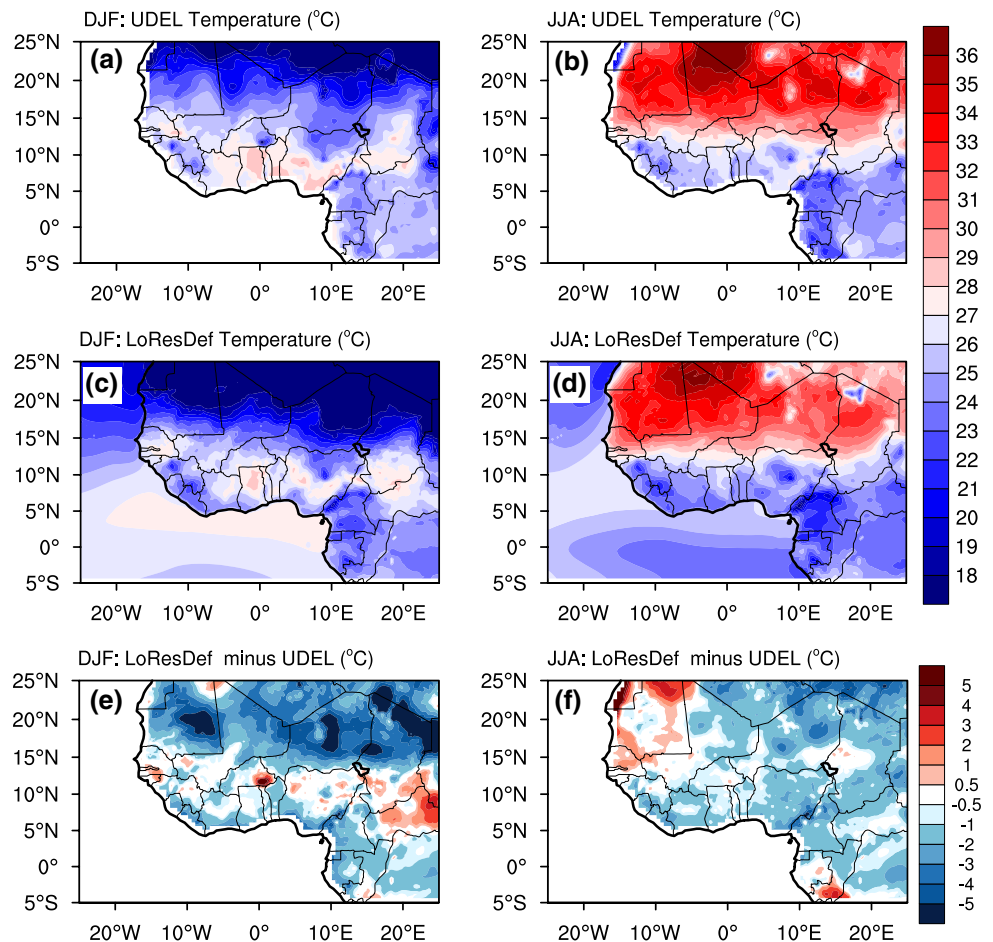
3 Results and discussion

Before analyzing the impact of the higher quality and finer resolution land cover distribution over West Africa, we first assess the performance of the regional climate model MD and LoResDef experiments in simulating seasonal and annual cycle of precipitation and temperature.

### 3.1 Simulated temperature and precipitation

To evaluate the simulated temperature and precipitation of the WAM annual cycle, a time-latitude Hovmoller diagram, along with some spatial and seasonal distributions, is adopted. This meridional cross-section analysis averaged from 15W to 15E provides a good framework to assess the regional climate model skill in simulating mean annual cycle and intra-seasonal variations of the WAM and associated mechanisms responsible for the rainfall variability (Hourdin et al. 2010; Sylla et al. 2013a).

As demonstrated by the time-latitude Hovmoller diagram of UDEL temperature observations averaged over the region 15E to 15E (Fig. 3a), the Sahara desert experiences

its warmest temperatures (>35 °C) during boreal summer and coldest temperatures during the boreal winter (~25 °C). The Gulf of Guinea, in contrast, experiences relatively lower and uniform temperatures throughout the year with a maximum of 25 °C in the boreal spring associated with the pre-monsoon season and a minimum of 23 °C during the peak monsoon season. The Sahel serves as a transition between the two regions. The temperature maximum in the Sahara, known as the Sahara Heat Low, intensifies and migrates northward from the northern Sahel in April–May to the Sahara in July–August. This migration initiates a progressive increase in meridional surface air temperature gradient that strengthens and shifts northwards the features triggering and maintaining the WAM which ultimately favors intense convection and precipitation in the Sahel (Mohr and Thorncroft 2006; Steiner et al. 2009; Sylla et al. 2010).

LoResDef exhibits close agreement in simulating the intensification and northward shift of the Sahara Heat Low (Fig. 3b); however, a notable cold bias is present throughout the entire year (Fig. 3c). The largest bias (~−4 °C) is simulated in northern Sahel and the Sahara desert at the

Fig. 5 Time-Latitude Hovmoller diagram of daily precipitation (mm/day) considering a 10-day running mean averaged for the period 1998–2010 and between 15E to 15N for TRMM (*upper panel*), LoResDef (*middle panel*) and the bias (LoResDef minus TRMM: *lower panel*)
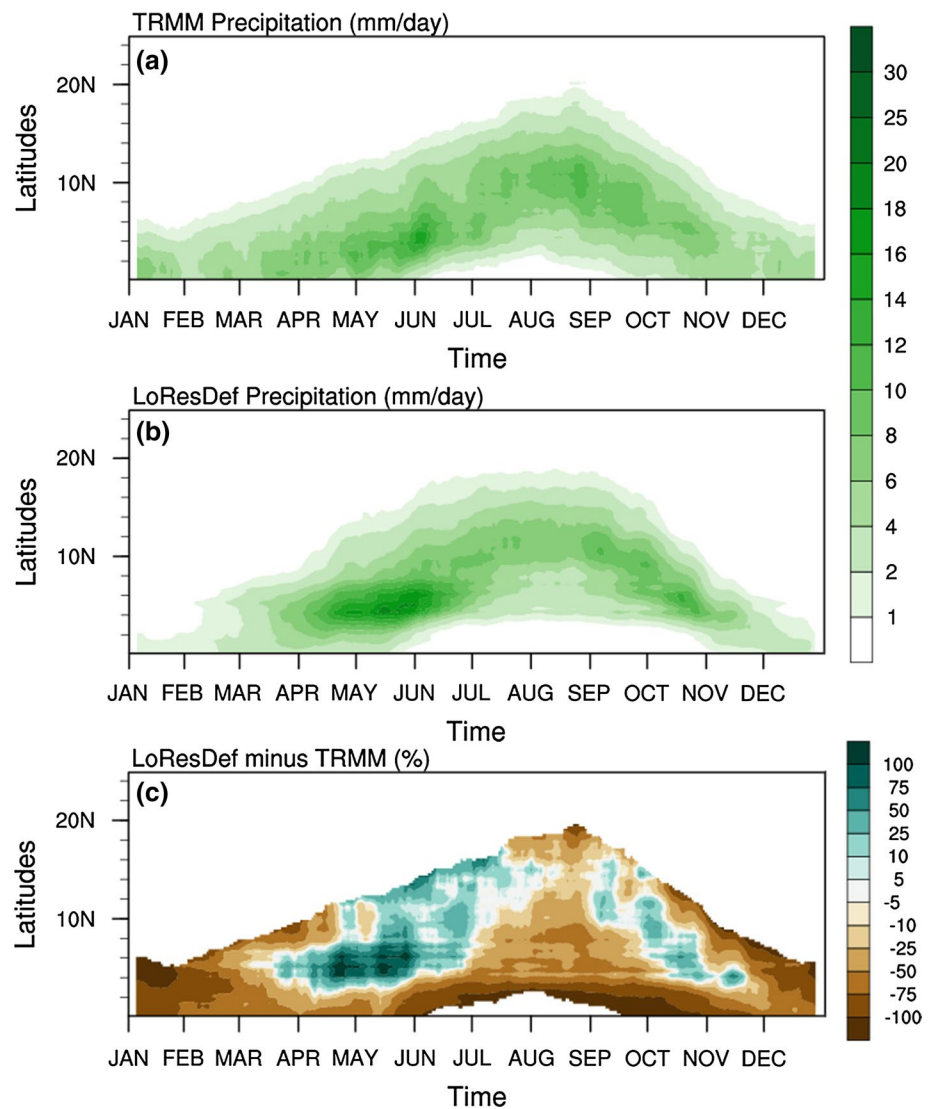

beginning (January–March) and the end (November–December) of the annual cycle. The smallest bias (<−2 °C) occurs during the peak of the monsoon season.

This is confirmed in Fig. 4 providing indications about the mean seasonal behavior of the spatial distribution of temperature averaged for December, January, and February (DJF) and June, July, and August (JJA). Figure 4 indicates that the general seasonal and spatial patterns are overall well simulated by the regional model. For instance, in DJF the relative positions of the coolest temperatures (<25 °C) observed in the Guinea Highlands, Jos Plateau and Cameroon Mountains and warmer temperatures (>28 °C) observed in Ghana, Benin, and Southern Nigeria are well captured. Also for the JJA season, warm temperatures occurring over most of West Africa with the highest values along the Sahel band and the Sahara desert between 10N and 25N and coolest temperature occurring along the Gulf of Guinea are reasonably simulated. Analysis of spatial

bias largely corroborates results from the Hovmoller diagram and reveals that the cold bias is more tied to the desert areas and the coastlines along the Gulf of Guinea. Such a cold bias can originate from a number of factors including an inaccurate representation of surface albedo, vegetation distribution, cloud radiative forcing and partitioning of net solar and longwave radiation into latent and sensible heat (Jones et al. 1995; Hudson and Jones 2002; Konaré et al. 2008; Sylla et al. 2012a; Giorgi et al. 2012).

Similar to temperature, time-latitude Hovmoller diagrams of the observed and simulated WAM precipitation are considered in Fig. 5. In this case, daily precipitation data is used to better characterize the annual cycle. To filter out the high-frequency variability, a 10-day running mean is applied to the daily time series. The TRMM data clearly display the three distinct phases of the annual cycle: the initiation or onset phase (March–May), the high rain period (JJA), and the southward retreat of the rainbelt

Fig. 6 Mean December–February (DJF: *left panel*) and June–August (JJA: *middle panel*) precipitation (mm/day) for the period 1998–2010 from TRMM (*upper panel*), LoResDef (*middle panel*) and their bias (LoResDef minus TRMM: *lower panel*)
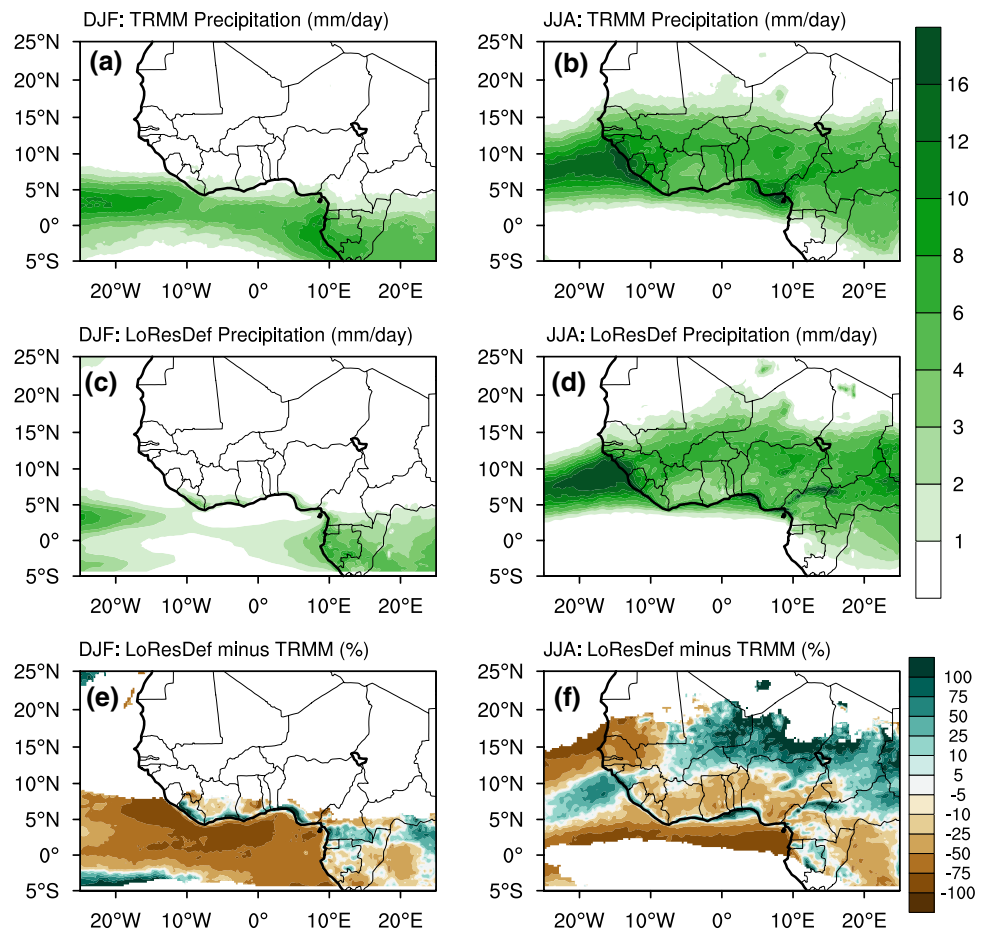
Table 1 Temperature mean bias (in °C) with respect to UDEL over different homogeneous subregions and West Africa

	Gulf of Guinea		Sahel		West Africa	
CRU	−0.14	−0.01	−0.01	0.19	−0.05	0.07
ERA-I	−0.18	−0.71	−0.16	0.15	−0.10	−0.41
MD	−1.71	−1.10	−0.55	1.30	−1.01	0.49
LoResDef	−1.11	−1.17	−0.76	−0.66	−0.85	−1.05
HiResNew	−1.01	−0.91	−0.70	−0.59	−0.80	−1.0

For each subregion, the 1st column is for DJF season, the second represents JJA

Table 2 Temperature pattern correlation coefficient with respect to UDEL over different homogeneous subregions and West Africa

	Gulf of Guinea		Sahel		West Africa	
CRU	0.89	0.87	0.80	0.97	0.86	0.97
ERA-I	0.83	0.77	0.75	0.97	0.79	0.95
MD	0.82	0.81	0.67	0.90	0.63	0.92
LoResDef	0.80	0.85	0.72	0.92	0.74	0.92
HiResNew	0.76	0.88	0.71	0.96	0.73	0.93

For each subregion, the 1st column is for DJF season, the second represents JJA

(September–October). The onset period is characterized by a northward extension of the rainbelt from the coast to about 4N. An abrupt shift, the monsoon jump, occurs at the beginning of June when the rain core moves rapidly northward to about 10N (Sultan and Janicot 2003). This is the beginning of the high rain season in Sahel region and the

Table 3 Precipitation mean bias (in %) with respect to TRMM over different homogeneous subregions and West Africa

	Gulf of Guinea		Sahel		West Africa	
UDEL	−20.13	−11.36	99.68	2.75	−22.34	−6.0
CRU	−44.48	−1.77	−52.79	0.26	−49.32	−2.19
ERA-I	97.36	2.39	−30.18	−41.79	91.56	−17.58
MD	18.06	28.83	58.31	−10.57	19.89	11.02
LoResDef	−34.99	−14.02	54.24	6.69	−30.93	−9.66
HiResNew	13.66	−2.88	60.98	8.59	60.05	6.37

For each subregion, the 1st column is for DJF season, the second represents JJA

Table 4 Precipitation pattern correlation coefficient with respect to TRMM over different homogeneous subregions and West Africa

	Gulf of Guinea		Sahel		West Africa	
UDEL	0.92	0.86	0.53	0.96	0.95	0.92
CRU	0.92	0.88	0.62	0.98	0.95	0.93
ERA−I	0.83	0.84	0.62	0.92	0.88	0.85
MD	0.48	0.64	0.40	0.68	0.63	0.72
LoResDef	0.40	0.75	0.49	0.66	0.54	0.70
HiResNew	0.40	0.75	0.47	0.69	0.53	0.72

For each subregion, the 1st column is for DJF season, the second represents JJA
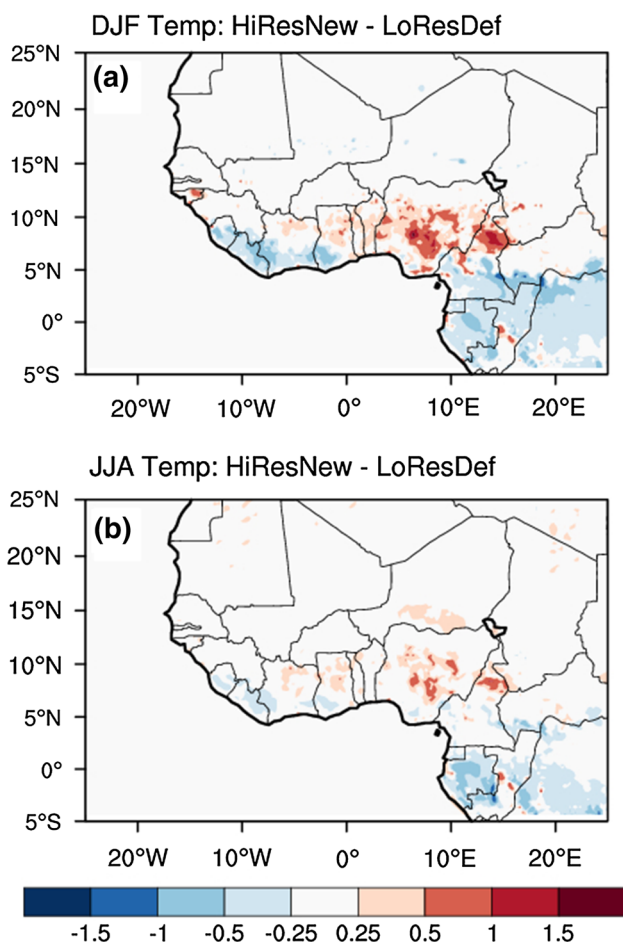
Fig. 7 Mean December–February (DJF: *upper panel*) and June–August (JJA: *lower panel*) Temperature differences (°C) between HiResNew and LoResDef

abrupt termination of heavy precipitation along the Guinea Coast. In September, a gradual southward retreat of the rainfall belt occurs, corresponding to the last phase of the WAM annual cycle.

Compared to the TRMM data, the three distinct phases of the mean annual cycle are well simulated by LoResDef. However, a number of differences are observed with regard to the magnitude and spatial extent of the features. For instance LoResDef shows a drier monsoon season and a wetter pre-monsoon and post-monsoon seasons over the Sahel. In the lower latitudes of the Gulf of Guinea, in contrast, a persistent dry bias prevails throughout the entire annual cycle.

Considering the spatial variability of precipitation (Fig. 6), the model captures the basic seasonal large-scale patterns. For instance, during the boreal winter season (DJF), both observed and simulated precipitation are confined in the lower latitudes, while regions north of 5°N are predominantly dry. However in JJA, the rain-band migrates to the Sahel where the Intertropical Convergence Zone (ITCZ) is at its northernmost location. Maximum precipitation occurs along the monsoon belt with intensity decreasing to the south and north. Additionally, precipitation maxima are located in topographically complex regions of Guinea Highlands, Jos Plateau and Cameroon Mountains while dry conditions are experienced in regions north of 20°N. Less intense precipitation, however, is simulated at the core of the ITCZ and more fine-scale features exist in the presence of complex topography. Additionally, a considerable dry bias is present along the Gulf of Guinea and western Sahel and a wet bias along the eastern Sahel during JJA. This bias
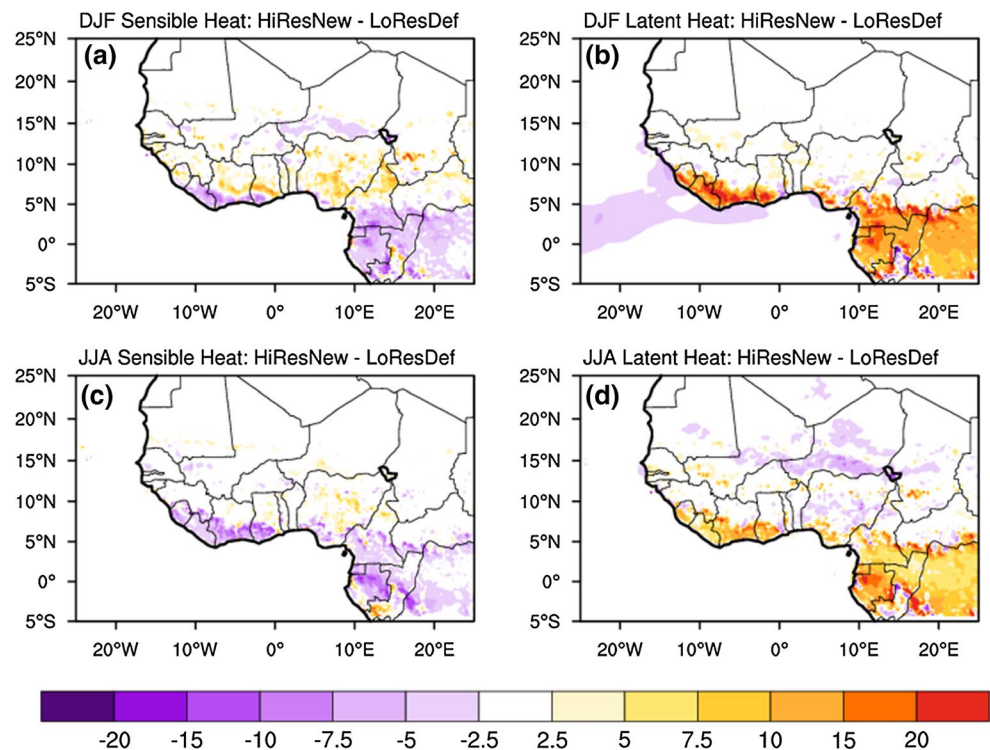
appears to correspond to a sharper definition of the ITCZ in the regional climate model.

To further assess the model performance at the regional scale and to highlight possible added value of LoRes-Def with respect to MD, biases and PCCs are computed for the Gulf of Guinea, the Sahel, and all of West Africa (Tables 1, 2, 3, 4). Temperature differences from CRU and ERA-Interim with respect to UDEL during DJF and JJA ranges from −0.14 to 0.2 °C and from −0.71 °C to 0.15 °C respectively and correlation coefficients exceeds 0.8 in most cases. This indicates a good level of agreement in the observed but also reanalyzed temperature patterns. In addition, the MD bias appears to be lower than ERA-Interim except in JJA over the Sahel and whole West Africa. A comparison between LoResDef and MD shows that the nested simulation exhibits a lower mean bias during DJF in the Gulf of Guinea and JJA in the Sahel and a greater PCC in most cases.

Similarly, Tables 3 and 4 reveals that in general, high correlation coefficients in the precipitation field (exceeding 0.8) are found between TRMM and CRU, UDEL and ERA-Interim. However, considerable differences are found in the magnitude of the precipitation. For instance CRU and UDEL appear to be substantially drier than TRMM in the Gulf of Guinea and whole West Africa for all seasons and a bit wetter in Sahel during JJA highlighting thus the uncertainty observed in different precipitation products due to the lack of precipitation gauges for ground truthing (Nikulin et al. 2012; Sylla et al. 2013b). Additionally, LoResDef

underestimates precipitation in the Gulf of Guinea (−35 % in DJF and −14 % in JJA) and West Africa (−31 % in DJF and −10 % in JJA) and overestimates in the Sahel (54 % in DJF and 7 % in JJA). In contrast, however, MD overestimates precipitation in all regions and seasons except in JJA in the Gulf of Guinea. PCC for all seasons and all regions are either comparable in magnitude or slightly greater in LoResDef than in MD. This implies that although the nested simulation may provide a slightly better spatial pattern than the mother domain, improvement in model performance is not systematic and is probably tied to the mature phase of the monsoon season in JJA. It should be noted that these model performances characterized by relatively substantial biases in precipitation are generally in line with the state-of-the-art regional climate models previously studied over West Africa (Nikulin et al. 2012; Sylla et al. 2013a; Gbobaniyi et al. 2014; Klutse et al. 2014). Note that the large magnitude of relative bias (in %) in DJF (Table 3) is more a reflection of precipitation being low than mean bias being high.

In summary, with a relatively coarse resolution (50 km), RegCM4 exhibits good performance in simulating the main characteristics of the WAM precipitation and temperature. However, at higher resolution (25 km), this performance is downgraded mostly in the Gulf of Guinea. The relatively small resolution increase (50–25-km) is likely not able to compensate the errors introduced by the nesting process inherent in regional climate modeling. Other errors may come through the increase of resolution itself because of the hydrostatic nature of the regional
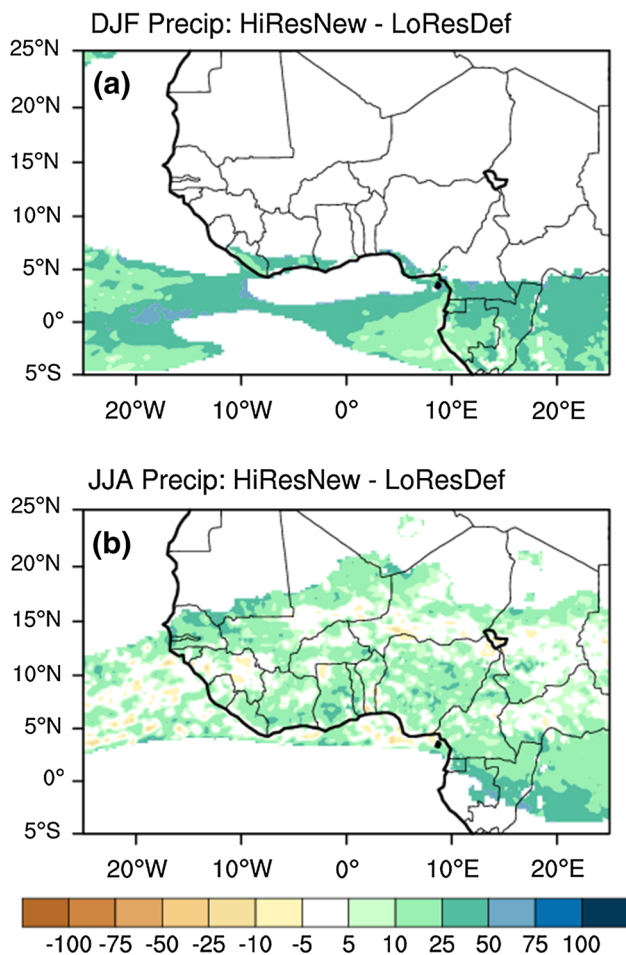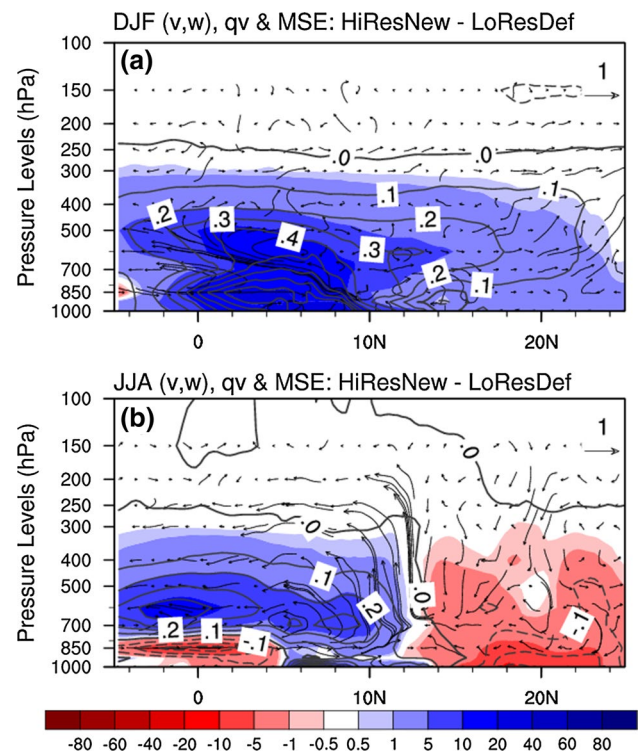
Fig. 9 Mean December–February (DJF: *upper panel*) and June–August (JJA: *lower panel*) precipitation differences (%) between HiResNew and LoResDef

Fig. 10 Latitude-Height cross-section of December–February (DJF: *upper panel*) and June–August (JJA: *lower panel*) water vapor mixing ratio with superimposed wind vectors in the (v, w) plane and moist static energy

model. In addition, RegCM4 settings are optimized at 50-km (Giorgi et al. 2012) and therefore, using it at 25-km without any additional fine-tuning can also introduce some errors. In fact, under the same land cover/land use conditions as the 50-km mother domain, the 25-km nested simulation is cooler and dryer over most West African regions. In the next section, we examine how the provision of higher resolution and improved PFT data modifies such deficiencies and highlight the underlying driving features and processes.

3.2 Impact of improved land cover distribution

The nested simulation using higher resolution improved land cover distribution (HiResNew) results in substantial changes in surface air temperature (Fig. 7). In particular, the conversion of grass into corn in central Nigeria, northern Cameroon, northern Gulf of Guinea and southern Niger leads to 0.25–1 °C of warming; and the increased broadleaf

evergreen trees results in similar magnitudes of cooling along the Gulf of Guinea coastal areas and central Africa. The magnitudes of the changes tend to be greater in DJF than in JJA, indicating that the summer monsoon precipitation tends to offset the effects of local vegetation distribution on surface air temperature.

The partitioning of net radiation into fluxes of sensible and latent heat largely controls the changes in temperature (Fig. 8). Changes in sensible heat flux are as large as 20 W/m^2 and coincide with the largest changes in surface temperature. In areas where temperature increases (decreases), sensible heat flux tends to increase (decrease). Similarly, increased (decreased) latent heat flux tends to occur in areas of cooling (warming) due to evaporative cooling. These changes are simulated in both DJF and JJA, implying that they are mostly tied to changes in local vegetation distribution. The response, however, during the monsoon season tends to be dampened likely due to the presence of saturated soil condition and resulting evapotranspiration amounts close to the potential regardless of the land cover type.

It is thus clear that the different plant types exhibit different responses of surface air temperature with corn tending to result in warming and trees cooling. In terms of model
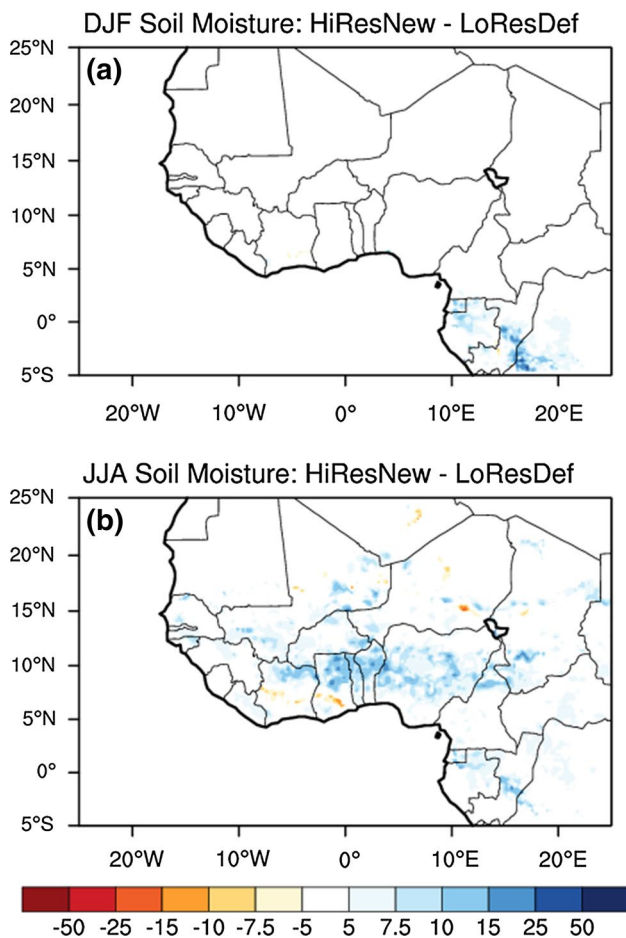
Fig. 11 Mean December–February (DJF: *upper panel*) and June–August (JJA: *lower panel*) total soil moisture (*left panel*) and surface runoff (*right panel*) differences (%) between HiResNew and LoResDef

regional temperature bias, these modifications reduce the model bias in the Gulf of Guinea, Sahel, and the entire West Africa when compared to the simulation with default land cover dataset (LowResDef) (Table 1). The largest improvements are simulated in Gulf of Guinea where the summer seasonal temperature bias is reduced from −1.2 to −0.9 °C. The improvements are smaller (probably due the smoothing of the area average) but consistent in the Sahel and entire West Africa where the summer seasonal biases are reduced slightly (from −0.7 to −0.6 °C and −1.05 to −1 °C, respectively).

Of particular interest is the response of monsoon precipitation to the changes in landcover distribution. Conversion of grass into corn and increased broadleaf evergreen tropical tree coverage both tend to lead to more precipitation over Central Nigeria, Gulf of Guinea, western Sahel and Central Africa (Fig. 9). This increase in precipitation occurs due to enhanced lower-level convergence and consequently stronger upward motions in land areas below 15N

during both DJF and JJA (Fig. 10). These conditions are consistent with the lager amount of simulated water vapor in the region, explaining thus the increases in monsoon precipitation. Such dynamic is favored by a net increase in Moisture Static Energy (MSE) from the surface to the mid levels during both seasons indicating more instabilities above the regions of vegetation changes. Also, consistent to precipitation and to some extent latent heat changes, the finer-resolution improved land cover distribution produces wetter soil conditions over most land areas sustaining thus the precipitation increase via a stronger soil moisture feedback (Fig. 11). The increased precipitation reduces the dry bias in the Gulf of Guinea and West Africa as a whole, but increases the wet bias simulated in Sahel (Table 3).

Whether these increases are due to the frequency (days with precipitation >1 mm) and/or the intensity of precipitation events is examined (Fig. 12). In DJF, increases in the frequency and intensity of precipitation events occur only in the lower latitudes tied the Gulf of Guinea coastlines and Central Africa. However in JJA, changes are more heterogeneous. In fact compared to LoResDef, HiResNew exhibits more frequent precipitation events in Western Sahel, a small portion of the Gulf of Guinea, and Central Africa; and higher precipitation intensity in Central Nigeria, some portions of the Gulf of Guinea and Sahel, and over Central Africa. These changes suggest that increased broadleaf evergreen tropical tree coverage favors an increase in both intensity and frequency of precipitation. However, in regions where corn dominates, such as central Nigeria, the precipitation increase is primarily due to an increase in precipitation intensity.

Overall, the changes induced by the higher resolution and higher-quality PFT data enhance to some extent the performance of the high resolution regional climate model in simulating temperature and precipitation in West Africa. The improved simulated temperature is due primarily to changes in turbulent heat fluxes, which causes an overall warming over most areas. The increased and somewhat improved precipitation is likely due to increased lower-level convergence and enhanced soil moisture feedback.

4 Conclusion

It is well established that West Africa is a region of strong land–atmosphere coupling, likely due to the sensitivity of the summer monsoon circulation to soil moisture and lower-level meridional temperature gradients. Modification of surface conditions can thus have considerable effects on the regional climate. In this study, the impact of higher resolution and improved land cover distribution is investigated over West Africa using RegCM4.3 coupled with CLM3.5. Model results are compared to those simulated with the
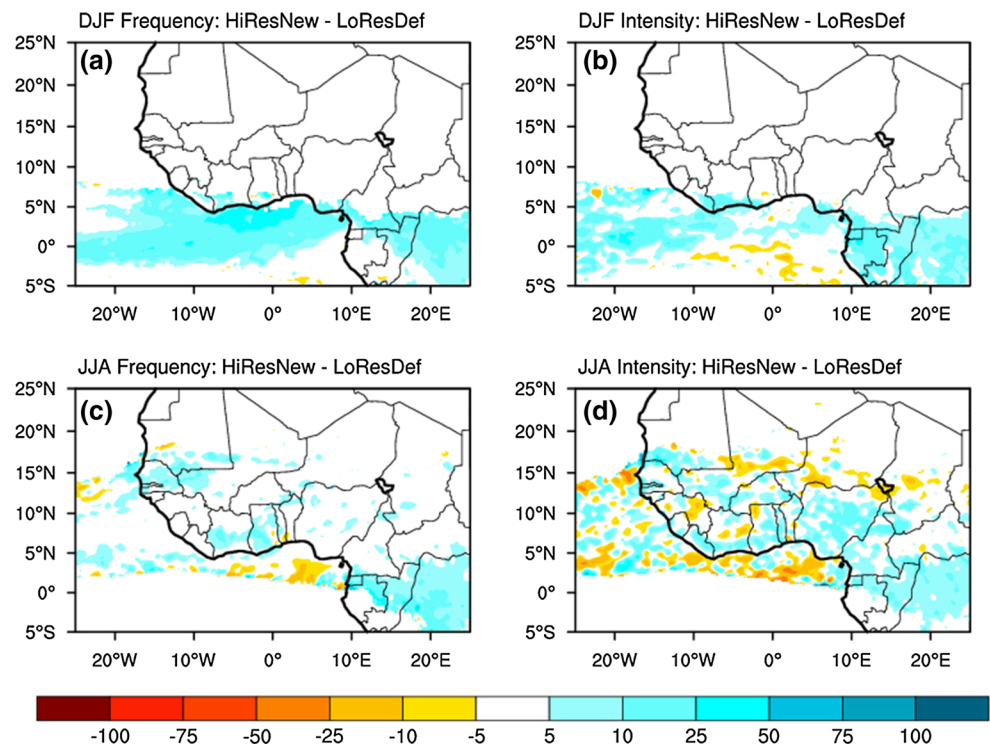
default coarser resolution PFT data present in CLM3.5. Key differences between the two sets of vegetation distribution are that the higher resolution improved PFT data replaces most of the C4 and C3 Grasses with corn and tropical broadleaf evergreen trees in most parts of West and Central Africa. The other land cover distribution remains relatively similar between the datasets. Both experiments, performed at high resolution (25 km) over West Africa, are driven by atmospheric data generated by the model at 50 km over a "mother domain" encompassing all of Africa.

The simulations reproduce the most prominent observed temperature and precipitation features of the West African monsoon. There, however, tends to be a cold bias over much of West Africa and a northward displacement of the monsoon. It should be emphasized that although the patterns are similar between all of the simulations, the biases are of different magnitude and spatial extent. Of particular importance, the simulation implementing the higher resolution updated PFT data, results in reduced temperatures biases and to some extent precipitation biases, highlighting the importance of high-quality vegetation data in West Africa.

Key processes leading to the moderately improved performance include partitioning of surface radiation into latent and sensible heat, which modifies atmospheric humidity and circulation. In regions where grass is converted to corn (central Nigeria, northeastern Sahel and northern Gulf of Guinea), sensible heat flux increases at the expense of latent heat flux. Conversely, in regions where grass is converted to broadleaf evergreen trees (central Africa and along the coastal areas of the Gulf of Guinea), latent heat flux increases at the expense of sensible heat flux. Therefore, conversion of grass into corn tends to result in warming conversion to broadleaf tends to result in cooling. While the presence of corn and broadleaf evergreen trees induce temperature changes opposite in sign, the precipitation change is mostly positive for both. In fact, wetter conditions are simulated over most of the domain even where changes in land cover are negligible. This originates from an increased lower-level convergence favoring stronger updrafts resulting in the presence of more atmospheric water vapor above the surface and also at the mid and higher levels. These conditions are primarily driven by the presence of more MSE indicating more atmospheric instabilities in regions of vegetation changes.

These results have important implications for regional climate and land surface modeling and also for West African afforestation, agricultural expansion and in general landuse/land cover politics. Accurate and high resolution land cover conditions are required for a realistic simulation of the WAM precipitation and temperature. In addition, large-scale removal of grass for corn agricultural expansion could slightly amplify the regional warming associated with anthropogenic climate change while afforestation of broadleaf evergreen tropical trees could mitigate it. Therefore, the results presented here indicate that the impact of land cover distribution should be accounted for in climate model experiments considering climate change over West Africa.

References

Abiodun BJ, Pal JS, Afiesimama EA, Gutowski WJ, Adedoyin A (2008) Simulation of West African monsoon using the RegCM3. Part II: impact of deforestation and desertification. Theor Appl Climatol 93(3–4):245–261. doi:10.1007/s00704-007-0333-1

Abiodun BJ, Adeyema DZ, Oguntunde PG, Salami AT, Ajayi VO (2012) Modeling the impact of reforestation on future climate in West Africa. Theoret Appl Climatol 110(1–2):77–96. doi:10.1007/s00704-012-0614-1

Abiodun BJ, Pal J, Afiesimama, EA, Gutowski WJ, Adedoyin A (2010) Modelling the impacts of deforestation on Monsoon Rainfall in West Africa. In: IOP conference series and environmental science vol. 13. doi:10.1088/1755-1315/13/1/012008

Afiesimama AE, Pal JS, Abiodun BJ, Gutowski WJ, Adedoyin A (2006) Simulation of West African monsoon using the RegCM3. Part I: model validation and interannual variability. Theor Appl Climatol 86:23–37. doi:10.1007/s00704-005-0202-8

Alo CA, Wang G (2010) Role of vegetation dynamics in regional climate predictions over western Africa. Clim Dyn 35(5):907–922. doi:10.1007/s00382-010-0744-z

Bounoua L, DeFries RS, Collatz GJ, Sellers PJ, Khan H (2002) Effects of land cover conversion on surface climate. Clim Change 52:29–64

Cook KH (1999) Generation of the African easterly jet and its role in determining West African precipitation. J Clim 12:1165–1184

Cretat J, Pohl B, Richard Y, Drobinski P (2012) Uncertainties in simulating regional climate of Southern Africa: sensitivity to physical parameterizations using WRF. Clim Dyn 38(3–4):613–634. doi:10.1007/s00382-011-1055-8

Dee and co-authors (2011) The ERA-Interim reanalysis: configuration and performance of the data assimilation system. Q J R Meteorol Soc 137:553–597. doi:10.1002/qj.828

Diallo I, Sylla MB, Giorgi F, Gaye AT, Camara M (2012) Multimodel GCM-RCM ensemble based projections of temperature and precipitation over West Africa for the early 21st century. Int J Geophys. doi:10.1155/2012/972896

Diallo I, Sylla MB, Camara M, Gaye AT (2013) Interannual variability of rainfall over the Sahel based on multiple regional climate models simulations. Theor Appl Climatol 113(1–2):351–362. doi:10.1007/s00704-012-0791-y

Diro GT, Raischer SA, Giorgi F, Tompkins AM (2012) Sensitivity of seasonal climate and diurnal precipitation over Central America to land and sea surface schemes in RegCM4. Clim Res 52:31–48. doi:10.3354/cr01049

Emanuel KA (1991) A scheme for representing cumulus convection in large-scale models. J Atmos Sci 48:2313–2335

Feddema JJ, Oleson KW, Bonan GB, Mearns LO, Buja LE, Meehl GA, Washington WM (2005) The importance of land-cover change in simulating future climates. Science 310(5754):1674–1678. doi:10.1126/science.1118160

Fontaine B, Trazaska S, Janicot S (1998) Evolution of the relationship between near and global and Atlantic SST modes and the rainy season in West Africa: statistical analyses and sensitivity experiments. Clim Dyn 14:353–368

Gbobaniyi E, Sarr A, Sylla MB, Diallo I, Lennard C, Dosio A, Dhiédiou A, Kamga A, Klutse NAB, Hewitson B, Nikulin G, Lamptey B (2014) Climatology, annual cycle and interannual variability of precipitation and temperature in CORDEX simulations over West Africa. Int J Climatol 34:2241–2257. doi:10.1002/joc.3834

Giannini A, Saravanan R, Chang P (2003) Oceanic forcing of Sahel rainfall on interannual to interdecadal time scales. Science 302:1027–1030. doi:10.1126/science.1089357

Giorgi F, Coppola E, Solmon F, Mariotti L, Sylla MB, Bi X, Elguindi N, Diro GT, Nair V, Giuliani G, Turuncoglu UU, Cozzini S, Güttler I, O'Brien TA, Tawfik AB, Shalaby A, Zakey AS, Steiner AL, Stordal F, Sloan LC, Brankovic C (2012) RegCM4: model description and preliminary tests over multiple CORDEX domains. Clim Res 52:7–29. doi:10.3354/cr01018

Grell GA (1993) Prognostic evaluation of assumptions used by cumulus parameterizations. Mon Weather Rev 121:764–787

Harris I, Jones PD, Osborn TJ, Lister DH (2014) Updated high-resolution grids of monthly climatic observations—the CRU TS3.10 Dataset. Int J Climatol 34:623–642. doi:10.1002/joc.3711

Holtslag AAM, De Bruin EIF, Pan HL (1990) A high resolution air mass transformation model for short-range weather forecasting. Mon Weather Rev 118:1561–1575

Hourdin F, Mustat I, Guichard F, Ruti PM, Favot F, Pham MMA, Grandpeix JY, Polcher J, Marquet P, Boone A, Lafore JP, Redelsperger JL, Dell'Aquilla A, Losada Doval T, Traore AK, Gallee H (2010) AMMA-Model intercomparison project. Bull Am Meteorol Soc 91:95–104. doi:10.1175/2009BAMS2791.1

Hsieh JS, Cook K (2005) Generation of African easterly wave disturbances: relationship to the African easterly jet. Mon Weather Rev 133:1311–1327

Hudson DA, Jones R (2002) Regional climate model simulations of present-day and future climates of southern Africa. Technical Note 39. Hadley Centre for Climate Prediction and Research, Met Off Bracknell, England

Huffman GJ, Bolvin DT, Nelkin EJ, Wolff DB, Adler RF, Gu G, Hong Y, Bowman KP, Stocker EF (2007) The TRMM multisatellite precipitation analysis (TMPA): Quasi-global, multiyear, combined-sensor precipitation estimates at fine scales. Journal of Hydrometeorology 8:38–55

Jenkins GS, Gaye AT, Sylla B (2005) Late 20th century attribution of drying trends in the Sahel from the regional climate model (RegCM3). Geophys Res Lett 32:L22705. doi:10.1029/2005GL024225

Jones RG, Murphy JM, Noguer M (1995) Simulation of climate change over Europe using a nested regional climate model I: assessment of control climate, including sensitivity to location of lateral boundary conditions. Q J R Meteorol Soc 121:1413–1449

Kiehl JT, Hack JJ, Bonan GB, Boville BA, Briegleb BP, Williamson DL, Rasch PJ (1996) Description of the NCAR Community Climate Model (CCM3). NCAR Tech. Note 4201STR, p 152

Klutse NAB, Sylla MB, Diallo I, Sarr A, Dosio A, Diedhiou A, Kamga A, Lamptey B, Ali A, Gbobaniyi EO, Owusu K, Lennard C, Hewitson B, Nikulin G, Panitz H, Buchner M (2014) Daily characteristics of West African monsoon rainfall in CORDEX regional climate models. Theor Appl Climatol. doi:10.1007/s00704-014-1352-3

Konaré A, Zakey AS, Solmon F, Giorgi F, Rauscher S, Ibrah S, Bi X (2008) A regional climate modeling study of the effect of desert dust on the West African monsoon. J Geophys Res 113:D12206. doi:10.1029/2007JD009322

Koster RD et al (2004) Regions of strong coupling between soil moisture and precipitation. Science 305:1138–1140

Kueppers LM, Snyder MA, Sloan LC (2007) Irrigation cooling effect: regional climate forcing by land-use change. Geophys Res Lett 34:L03703. doi:10.1029/2006GL028679

Kummerow C, Hong Y, Olson WS, Yang S, Adler RF, McCollum J, Ferraro R, Petty G, Shin DB, Wilheit TT (2001) The evolution of the Goddard profiling algorithm (GPROF) for rainfall estimation from passive microwave sensors. J Appl Meteorol 40:1801–1840

Lawrence PJ, Chase TN (2010) Investigating the climate impacts of global land cover change in the community climate system model. Int J Climatol 30:2066–2087. doi:10.1002/joc.2061

Legates DR, Willmott CJ (1990) Mean seasonal and spatial variability in gauge-corrected, global precipitation. Int J Climatol 10:111–127

Mohr KI, Thorncroft CD (2006) Intense convective systems in West Africa and their relationship to the African easterly jet. Q J R Meteorol Soc 132:163–176

Moufouma-Okia W, Rowell DP (2010) Impact of soil moisture initialisation and lateral boundary conditions on regional climate model simulations of the West African Monsoon. Clim Dyn 35:213–229. doi:10.1007/s00382-009-0638-0

Mounkaila SM, Abiodun BJ, Omotosho JB (2014) Assessing the capability of CORDEX models in simulating onset of rainfall in West Africa. Theor Appl Climatol. doi:10.1007/s00704-014-1104-4

Nikulin G, Jones C, Samuelsson P, Giorgi F, Asrar G, Büchner M, Cerezo-Mota R, Christensen OB, Déqué M, Fernandez J, Hänsler A, van Meijgaard E, Sylla MB, Sushama L (2012) Precipitation climatology in an ensemble of CORDEX-Africa regional climate simulations. J Clim. doi:10.1175/JCLI-D-11-00375.1

Oleson KW, Niu GY, Yang ZL, Lawrence DM, Thornton PE, Lawrence PJ, Stöckli R, Dickinson RE, Bonan GB, Levis S, Dai A, Qian T (2008) Improvements to the Community Land Model and their impact on the hydrological cycle. J Geophys Res 113:G01021. doi:10.1029/2007JG000563

Otieno VO, Anyah RO (2012) Effects of land use changes on climate in the Greater Horn of Africa. Climate Research 52:77–95

Paeth H, Born K, Podzun R, Jacob D (2005) Regional dynamical downscaling over West Africa: model evaluation and comparison of wet and dry years. Meteorol Z 14(3):349–367

Pal JS, Small EE, Eltahir EAB (2000) Simulation of regional-scale water and energy budgets: representation of subgrid cloud and precipitation processes within RegCM. J Geophys Res 105:29579–29594

Pal JS, Giorgi F, Bi X, Elguindi N, Solmon F, Gao X, Rauscher S, Francisco R, Zakey A, Winter J, Ashfaq M, Syed FS, Bell JL, Diffenbaugh NS, Karmacharya J, Konaré A, Martinez D, da Rocha RP, Sloan LC, Steiner AL (2007) The ICTP RegCM3 and RegCNET: regional climate modeling for the developing world. BAMS 88:1395–1409. doi:10.1175/BAMS-88-9-1395

Patricola CM, Cook KH (2008) Atmosphere/vegetation feedbacks: a mechanism for abrupt climate change over northern Africa. J Geophys Res 113:D18102. doi:10.1029/2007JD009608

Pohl B, Douville H (2011) Diagnosing GCM errors over West Africa using relaxation experiments. Part I: summer monsoon climatology and interannual variability. Clim Dyn 37:1293–1312. doi:10.1007/s00382-010-0911-2

Reynolds RW, Rayner NA, Smith TM, Stokes DC, Wang W (2002) An improved in situ and satellite SST analysis. J Clim 15:1609–1625

Rummukainen M (2010) State-of-the-art with regional climate models. Clim Change 1:82–86

Ruti PM, Williams JE, Hourdin F, Guichard F, Boone A, van Velthoven P, Favot F, Musat I, Rummukainen M, Dominguez M, Gaertner MA, Lafore JP, Losada T, de Fonseca MBR, Polcher J, Giorgi F, Xue Y, Bouarar I, Law K, Josse B, Barret B, Yang X, Mari C, Traore AK (2010) The West African climate system: a review of the AMMA model inter-comparison initiatives. Atmos Sci Lett 12:116–122. doi:10.1002/asl.305

Steiner AL, Pal JS, Rauscher SA, Bell JL, Diffenbaugh NS, Boone A, Sloan LC, Giorgi F (2009) Land surface coupling in regional climate simulations of the West African monsoon. Clim Dyn 33:869–892. doi:10.1007/s00382-009-0543-6

Sultan B, Janicot S (2003) The West African monsoon dynamics. Part II: the "preonset" and "onset" of the summer monsoon. J Clim 16:3407–3427

Sylla MB, Dell'Aquila A, Ruti PM, Giorgi F (2010) Simulation of the intraseasonal and the interannual variability of rainfall over West Africa with RegCM3 during the monsoon period. Int J Climatol 30:1865–1883. doi:10.1002/joc.2029

Sylla MB, Giorgi F, Ruti PM, Calmanti S, Dell'Aquila A (2011) The impact of deep convection on the West African summer monsoon climate: a regional climate model sensitivity study. Q J R Meteorol Soc 137:1417–1430. doi:10.1002/qj.853

Sylla MB, Giorgi F, Stordal F (2012a) Large-scale origins of rainfall and temperature bias in high resolution simulations over Southern Africa. Clim Res 52:193–211. doi:10.3354/cr01044

Sylla MB, Gaye AT, Jenkins GS (2012b) On the fine-scale topography regulating changes in atmospheric hydrological cycle and extreme rainfall over West Africa in a Regional Climate Model projections. Int J Geophys. doi:10.1155/2012/981649

Sylla MB, Diallo I, Pal JS (2013a) West African monsoon in state-of-the-science regional climate models, climate variability—regional and thematic patterns. In: Dr. Aondover Tarhule (Ed.), ISBN: 978-953-51-1187-0, InTech, doi:10.5772/55140

Sylla MB, Giorgi F, Coppola E, Mariotti L (2013b) Uncertainties in daily rainfall over Africa: assessment of gridded observation products and evaluation of a regional climate model simulation. Int J Climatol 33:1805–1817. doi:10.1002/joc.3551

van den Hurk BJJM, van Meijgaard E (2010) Diagnosing land-atmosphere interaction from a regional climate model simulation over West Africa. J Hydrometeorol 11:467–481. doi:10.1175/2009JHM1173.1

Wang G, Eltahir EAB (2000) Ecosystem dynamics and the Sahel drought. Geophys Res Lett 27(6):795–798

Xue Y, Juang HMH, Li W, Prince S, DeFries R, Jiao Y, Vasic R (2004) Role of land surface processes in monsoon development: East Asia and West Africa. J Geophys Res 109:D03105. doi:10.1029/2003JD003556

Xue Y, De Sales F, Lau KMW, Bonne A, Feng J, Dirmeyer P, Guo Z, Kim KM, Kitoh A, Kumar V, Poccard-Leclercq I, Mahowald N, Moufouma-Okia W, Pegion P, Rowell DP, Schemm J, Schubert S, Sealy A, Thiaw WM, Vintzileos A, Williams SF, Wu ML (2010) Intercomparison of West African monsoon and its variability in the West African monsoon modelling evaluation project (WAMME) first model intercomparison experiment. Clim Dyn 35:3–27. doi:10.1007/s00382-010-0778-2

Yu M, Wang G (2013) Impact of bias correction of lateral boundary conditions on regional climate projections in West Africa. Clim Dyn. doi:10.1007/s00382-013-1853-2

Zaroug MAH, Sylla MB, Giorgi F, Eltahir EAB, Aggarwal PK (2012) A sensitivity study on the role of the Swamps of Southern Sudan in the summer climate of North Africa using a regional climate model. Theoret Appl Climatol 113(1–2):63–81. doi:10.1007/s00704-012-0751-6

Zeng X, Zhao M, Dickinson RE (1998) Intercomparison of bulk aerodynamic algorithms for the computation of sea surface fluxes using TOGA COARE and TAO data. J Clim 11:2628–2644